RSMA-Integrated Full-Duplex Communications for Better Energy and Spectral-Efficiency Trade-off

Raviteja Allu[†], Mayur Katwe[†], Keshav Singh[†], Trung Q. Duong[‡], and Chih-Peng Li[†]
[†]Institute of Communications Engineering, National Sun Yat-sen University, Kaohsiung 804, Taiwan
[‡]School of Electronics, Electrical Engineering, and Computer Science, Queen's University Belfast, Belfast, U.K.
E-mail: {alluraviteja202, mayurkatwe}@gmail.com, keshav.singh@mail.nsysu.edu.tw, trung.q.duong@qub.ac.uk, cpli@faculty.nsysu.edu.tw

***Abstract*—This paper explores an unconventional physical-layer architecture, i.e., full-duplex (FD) integrated rate-splitting multiple access (RSMA) to attain a better trade-off between energy efficiency (EE) and spectral efficiency (SE) under multi-user scenarios. The considered FD-RSMA system divides and encodes the original messages of each downlink (DL) and uplink (UL) into multiple sub-messages, and later transmits them at the same resource block, resulting in strong inter-user interference and cross-link interference, i.e., self-interference (SI) and co-channel interference (CCI). Here, we focus on the multi-objective optimization (MOO) problem, i.e., jointly maximizing the EE and SE of the considered FD-RSMA system via joint power allocation for simultaneous UL and DL communication, subject to transmit power constraints and given quality of service (QoS) requirements. Firstly, the MOO problem is transformed into a single objective optimization (SOO) problem using the weighted sum method with a trade-off parameter. Subsequently, we adopt an iterative algorithm that employs inner approximation techniques to attain near-optimal resource allocation for the transformed SOO problem via effective interference management. Simulation results validate that the FD-RSMA scheme effectively outperforms counterpart multi-user precoding FD schemes like space-division multiple access (SDMA) and non-orthogonal multiple access (NOMA).**

***Index Terms*—Full-duplex (FD), rate-splitting multiple access technique (RSMA), spectral efficiency, energy efficiency.**

I. Introduction

The rapid proliferation of wireless devices and services has led to an exponential increase in demand for reliable and high-speed wireless communication networks [1]. Sixth-generation (6G) wireless networks are poised to enable a new paradigm of data services involving higher data rates, lower latency, and ultra-reliability under stringent power budgets which are beyond the capabilities of conventional multiple-access schemes [2]. This necessitates new disruptive physical layer strategies which ensure the acute realization of high system performance for multiple users under limited spectral and power resources. Undoubtedly, the growing concern for the high-system performance and the economic burden associated with power consumption necessitates the simultaneous consideration of spectral efficiency (SE) and energy efficiency (EE) as key performance metrics for 6G networks [3].

In recent years, full-duplex (FD) systems have been recognized as a prominent physical layer design technology that enables simultaneous transmission and reception of uplink and downlink traffic over the same resource block [4]. In particular, FD systems can approximately double the spectral efficiency compared to half-duplex (HD) systems operated on time-division or frequency-division duplexing. The experimental results on full-duplex real-time radios in [5] confirmed that FD systems achieve about 1.9 times higher throughput than HD systems. Nevertheless, the self-interference (SI) from transmit antennas to receive antennas constitutes a prime bottleneck for the application of FD systems [6]. The recent advancements in analog and digital processing techniques have effectively reduced SI to the background noise level, making FD communications more feasible.

Another frontier physical layer strategy, called rate-splitting multiple access (RSMA) techniques, has been envisaged as next-generation multiple access scheme in the past few years owing to its better interference management and power control policy when compared to conventional multi-user linear precoding (MU-LP), i.e., space division multiple access (SDMA), non-orthogonal multiple access (NOMA) and orthogonal multiple access (OMA) schemes [7]. In particular, RSMA splits the intended messages into multiple sub-messages and transmits them within the same frequency and time slot. It aims to improve overall system performance with respect to (w.r.t.) spectral efficiency [8], power minimization, user fairness [9], and reliability [10] through effective interference management and successive interference cancelation decoding scheme. Like in downlink (DL) RSMA, user messages are split into common and private parts and then encoded into separate streams using available channel state information at the transmitter. In uplink RSMA, a message from each uplink (UL) user is split into several sub-messages based on split proportions, where each part contributes to the rate of that user [11].

Using RSMA, the available resources can be efficiently split between users, leading to increased throughput. On the other hand, FD systems allow simultaneous transmission and reception, reducing the time required for data transmission and improving reliability. Interestingly, the interplay of an FD and RSMA system can lead to significant improvements in spectral efficiency, energy efficiency, latency, and network capacity for both UL and DL communication. While some literature demonstrates the excellence of NOMA-integrated FD systems [12], the exploration of RSMA with FD remains unexplored, despite RSMA's outperformance over NOMA. Notably, the occurrence of cross-interference in FD transmission can be a major bottleneck in the FD-RSMA scheme, which requires careful consideration. Thus, an optimal resource allocation

design for effective interference management in the FD-RSMA system is a compelling research topic, especially to achieve both energy and spectral efficiency, and it forms the primary motivation for this work.

Despite its advantages, the study on the integration of FD and RSMA system has not been sufficiently addressed remarkably in the literature. The work in [13] adopted an FD cooperative RSMA scheme where the strongest user among the two users was acting as an FD relay for the DL system; however, the RSMA operation of UL and DL transmission at the base station (BS) was not fully realized. The authors of [14] discussed the SE-EE trade-off problem in the RSMA-assisted downlink network and found a globally optimal solution, while the authors of [10] addressed the SE-EE trade-off problem considering the multi-objective optimization (MOO) problem. Indeed, optimal power control in the FD-RSMA system is a fundamental concern that involves a highly complex resource allocation problem and smart interference mitigation for UL and DL transmission. Nonetheless, to the best of the authors' knowledge, this is the first work that studies an RSMA-integrated FD system to achieve a spectral and energy-efficient multi-user communication system. The major contribution of the work is as follows:

1) Unlike [10], [14], we consider an RSMA-integrated FD architecture where a multi-antenna base station (BS) communicates with multiple single-antenna UL and DL users within the same time and frequency slot.
2) In particular, a MOO problem for SE-EE trade-off is formulated for the considered system under given transmit power and rate requirements constraints. To solve the formulated problem, we first transform it into an equivalent single-objective optimization problem and later solved it using a low-cost iterative method based on successive convex approximation (SCA).
3) Subsequently, simulation results are presented to validate the outperformance of the FD-RSMA system over conventional half-duplex, multi-user precoding schemes like SDMA and NOMA schemes.

II. System Model and Preliminaries

Let us consider a FD scenario where a base station (BS) consists of multiple transmit antennas (M_t) and receive antennas (M_r). Here, the BS simultaneously caters to D DL and U UL single-antenna users, as illustrated in Fig. 1. $\mathcal{U} \triangleq \{1 \dots U\}$, $\mathcal{D} \triangleq \{1 \dots D\}$, $\mathcal{R} \triangleq \{1 \dots M_r\}$ and $\mathcal{T} \triangleq \{1 \dots M_t\}$ are respectively the set of UL users, DL users, transmitting antennas and receiving antennas. For the sake of simplicity design and theoretical performance evaluation of the considered system, we strictly assume that the perfect channel state information for each link is known a prior. Denoting $\mathbf{g}_d^{DL} \in \mathbb{C}^{M_t \times 1}, d \in \mathcal{D}$ as the channel between BS to d^{th} DL user, $\mathbf{g}_u^{UL} \in \mathbb{C}^{1 \times M_r}, u \in \mathcal{U}$ as the channel between u^{th} UL user to BS, $h_{u,d} \in \mathbb{C}, u \in \mathcal{U}, d \in \mathcal{D}$ as the interference channel between u^{th} UL user to d^{th} DL user, and $\mathbf{F} \in \mathbb{C}^{M_t \times M_r}$ as the SI channel gain.

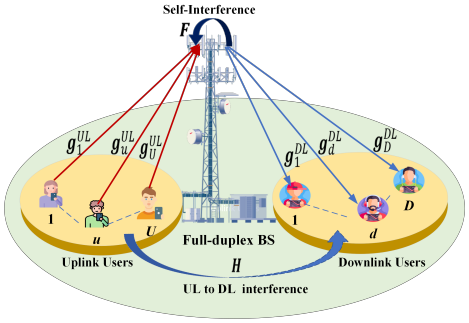

Fig. 1: An illustration of the FD RSMA system model.

In the considered FD-RSMA system, the BS transmits a set of original messages $\mathcal{W}^{DL} \triangleq \{W_1^{DL}, \dots, W_D^{DL}\}$ to the DL users such that the message of each d^{th} DL user, W_d^{DL}, is divided into two parts, i.e., the common and private sub-messages, respectively, which are denoted as $W_{d,\mathrm{c}}^{DL} \in \mathbb{C}$ and $W_{d,\mathrm{p}}^{DL} \in \mathbb{C}$, respectively such that $\mathrm{E}[W_{d,\mathrm{c}}^{DL}(W_{d,\mathrm{c}}^{DL})^H] = 1$ and $\mathrm{E}[W_{d,\mathrm{p}}^{DL}(W_{d,\mathrm{p}}^{DL})^H] = 1, \forall d \in \mathcal{D}$. In particular, the BS encodes all the common sub-messages of all the users into a common data stream s_{c}^{DL} and private sub-messages into the distinct dedicated data streams, $s_d^{DL}, \forall d$. So, the superimposed symbol of all DL users transmitted by BS is expressed as

$$\mathbf{x}_T = \mathbf{w}_c s_c^{DL} + \sum\nolimits_{k \in \mathcal{D}} \mathbf{w}_k s_k^{DL}, \tag{1}$$

where $\mathbf{w}_c \in \mathbb{C}^{M_t \times 1}$ and $\mathbf{w}_k \in \mathbb{C}^{M_t \times 1}, \forall\, k \in \mathcal{D}$ are the transmit beamformers for the common stream and for a private stream of d^{th} DL user, respectively.

Furthermore, each u^{th} UL user divides its original messages W_u^{UL} into two distinct sub-messages $W_{u,1}^{UL}$ and $W_{u,2}^{UL}$ such that $\mathrm{E}[W_{u,j}^{UL}(W_{u,j}^{UL})^H] = 1, \forall j \in \mathcal{J} \triangleq \{1, 2\}, \forall u \in \mathcal{U}$. These sub-messages are later encoded into distinct streams $s_{u,j}^{UL}, \forall u, \forall j$ and later transmitted by the BS. So, the transmitted signal by each u^{th} UL user is given as

$$x_u^{UL} = \sum\nolimits_{j \in \mathcal{J}} \sqrt{p_{u,j}} s_{u,j}^{UL}, \forall\, u \in \mathcal{U}, \tag{2}$$

where $p_{u,j} \in \mathbb{C}^{1 \times 1}, \forall\, u \in \mathcal{U},\ \forall\, j \in \mathcal{J}$ is the transmit power allocated to u^{th} UL user to transmit j^{th} sub message of that user.

The received signal at the d^{th} DL user is given as

$$\begin{aligned} y_d =& (\mathbf{g}_d^{DL})^{\mathrm{H}} \mathbf{x}_T + \sum\nolimits_{u \in \mathcal{U}} h_{d,u} \mathbf{x}_d^{UL} + \eta_d \\ =& (\mathbf{g}_d^{DL})^{\mathrm{H}} \mathbf{w}_c s_c^{DL} + (\mathbf{g}_d^{DL})^{\mathrm{H}} \sum_{i \in \mathcal{K}} \mathbf{w}_i s_i^{DL} \\ &+ \underbrace{\sum\nolimits_{u \in \mathcal{U}} \sum\nolimits_{j \in \mathcal{J}} h_{d,u} \sqrt{p_{u,j}} s_{u,j}^{UL}}_{\text{UDI}} + \eta_d^{DL}, \end{aligned} \tag{3}$$

where $\eta_d^{DL} \sim \mathcal{CN}\left(0, (\sigma_d^{DL})^2\right)$ is the additive white Gaussian noise (AWGN) with noise power of $(\sigma_d^{DL})^2$ at d^{th} DL user. Note that the signal received by the d^{th} DL user includes the desired signal from the BS, as well as interference from other DL users, known as inter-user interference (IUI), interference

from UL users, known as UL to DL users interference (UDI), and noise.

The overall signal received at BS can be expressed as

$$\boldsymbol{y}_{B} = \sum\nolimits_{u\in\mathcal{U}} \mathbf{g}_u^{UL} x_u^{UL} + \mathbf{F}^{\mathrm{H}}\mathbf{x}_T + \boldsymbol{\eta}_{B} \tag{4}$$

$$= \sum\nolimits_{u\in\mathcal{U}} \mathbf{g}_u^{UL} \sum\nolimits_{j\in\mathcal{J}} \sqrt{p_{u,j}} s_{u,j}^{UL} + \underbrace{\mathbf{F}^{\mathrm{H}}\left(\mathbf{w}_{c} s_{c}^{DL} + \sum\nolimits_{d\in\mathcal{D}} \mathbf{w}_{k} s_{d}^{DL}\right)}_{SI} + \boldsymbol{\eta}_{B}, \tag{5}$$

where $\boldsymbol{\eta_B} \sim \mathcal{CN}\left(\mathbf{0}, (\sigma_{BS}^{UL})^2 I_{M_r}\right)$ is the AWGN with noise power of $(\sigma_{BS}^{UL})^2$ at BS. Note that the received signal at the BS includes the sub-messages of UL users, SI from the transmit antennas of the BS, and the noise.

A. Achievable rate

For DL RSMA, the common stream sent by BS is firstly decoded at each DL user by treating all the private streams as interference (IUI) along with UDI and noise, and later using SIC at the DL user, the decoded common stream is subtracted from the received signal. So, the signal-to-interference-plus-noise ratio (SINR) of the common stream at d^{th} DL user is

$$\gamma_{\mathrm{c},d}^{DL} = \frac{|(\mathbf{g}_d^{DL})^{\mathrm{H}}\mathbf{w}_{\mathrm{c}}|^2}{\sum\limits_{i\in\mathcal{D}} |(\mathbf{g}_d^{DL})^{\mathrm{H}}\mathbf{w}_i|^2 + \sum\limits_{u\in\mathcal{U}}\sum\limits_{j\in\mathcal{J}} p_{u,j}^{UL}|h_{d,u}|^2 + (\sigma_{\mathrm{c},d}^{DL})^2}, \tag{6}$$

and the corresponding common rate is given as

$$R_{\mathrm{c},d}^{DL} = \log_2(1+\gamma_{\mathrm{c},d}^{DL}), \forall\, d\in\mathcal{D}. \tag{7}$$

Nevertheless, the rate of the common stream, denoted as R_{c}^{DL}, should be selected as the minimum among the common rates of all users to ensure that the common stream can be decoded successfully by all DL users, which follows

$$R_{\mathrm{c}}^{DL} = \min\{R_{\mathrm{c},1}^{DL} \ldots R_{\mathrm{c},D}^{DL}\} \tag{8}$$

Moreover, each private stream is decoded at the corresponding DL user treating other private streams as interference along with UDI and noise. The SINR to decode d^{th} private stream at the corresponding DL user is given as

$$\gamma_{\mathrm{p},d}^{DL} = \frac{|(\mathbf{g}_d^{DL})^{\mathrm{H}}\mathbf{w}_d|^2}{\sum\limits_{i\in\mathcal{D},i\neq d} |(\mathbf{g}_d^{DL})^{\mathrm{H}}\mathbf{w}_i|^2 + \sum\limits_{u\in\mathcal{U}}\sum\limits_{j\in\mathcal{J}} p_{u,j}^{UL}|h_{d,u}|^2 + (\sigma_d^{DL})^2}. \tag{9}$$

and the corresponding private rate is given by

$$R_{\mathrm{p},d}^{DL} = \log_2(1+\gamma_{\mathrm{p},d}^{DL}), \forall\, d\in\mathcal{D}. \tag{10}$$

Overall, the rate at d^{th} DL user is expressed as

$$R_{d,tot}^{DL} = C_d^{DL} + R_{\mathrm{p},d}^{DL}, \forall\, d\in\mathcal{D}. \tag{11}$$

where, C_d^{DL} is part of the common rate intended for d^{th} DL user such that $\sum_d C_d^{DL} = R_c^{DL}$.

For the UL, the BS decodes all sub-messages transmitted by UL users using SIC based on a predefined decoding order such that the first sub-messages of the decoding order is decoded first, followed by the second element and so on, the BS successfully decodes and eliminates all sub-messages with a decoding order lower than $s_{u,j}^{UL}$ and treats the remaining sub-messages as interference [15]. Similar to [15], we adopt the decoding order Π aiming to maximize user fairness such that

$$\Pi = \big\{(s_{u,j}^{Ul} \rightarrow s_{u',j}^{Ul} \rightarrow s_{u,j'}^{Ul} \rightarrow s_{u',j'}^{Ul}) : \left|\mathbf{g}_u^{UL}\right| \geq \left|\mathbf{g}_{u'}^{UL}\right|, l\neq u', u, u'\in\mathcal{U}, j, j'\in\mathcal{J}\big\}. \tag{12}$$

Without loss of generality, it is assumed that an efficient digital SI cancellation is employed; however, there still exists some part of SI due to hardware constraints [12] which is termed residual self-interference. Ultimately, the SINR for the $s_{u,j}^{Ul}$ of u^{th} user can be expressed as

$$\gamma_{u,j}^{UL} = \frac{p_{u,j}^{UL}|\mathbf{g}_u^{UL}\mathbf{z}_u|^2}{\sum\limits_{(m,n)\in\mathcal{Q}_{u,j}} p_{m,n}^{UL}|\mathbf{g}_m^{UL}\mathbf{z}_m|^2 + \left(P_{SI}+\sigma_{BS}^{UL^2}\right)||\mathbf{z}_u||^2}, \tag{13}$$

where $\mathbf{z}_u \in \mathbb{C}^{M_r\times 1}$ is the receive beamformer at the BS to decode the signal from the u^{th} UL user, $\mathcal{Q}_{u,j}$ is the set of all the messages which have higher decoding order than $s_{u,j}^{UL}$ and $P_{SI} = \omega(|\mathbf{F}^{\mathrm{H}}\mathbf{w}_{\mathrm{c}}|^2 + \sum_{d\in\mathcal{D}}|\mathbf{F}^{\mathrm{H}}\mathbf{w}_d|^2)$ such that ω is the RSI coefficient. Now, the overall rate for the u^{th} user is given as

$$R_u^{UL} = \sum\nolimits_{j\in\mathcal{J}} R_{u,j}^{UL} = \sum\nolimits_{j\in\mathcal{J}} \log_2(1+\gamma_{u,j}^{UL}), \forall\, u\in\mathcal{U}. \tag{14}$$

The spectral efficiency for the considered system is given as

$$SE = \sum\nolimits_{d\in\mathcal{D}} (C_d^{DL} + R_{\mathrm{p},d}^{DL}) + \sum\nolimits_{u\in\mathcal{U}} R_u^{UL}. \tag{15}$$

B. Power consumption model and Energy Efficiency

The total power consumption of the FD-RSMA system depends on the transmit power at the BS and the UL users and the constant power consumed by the circuitry denoted as P_C. The total power consumption of the system is given by

$$P_T = \frac{1}{\rho_d}\left(\sum_{k\in\mathcal{D}} |\mathbf{w}_k|^2 + |\mathbf{w}_{c}|^2\right) + \frac{1}{\rho_u}\sum_{u\in\mathcal{U}}\sum_{j\in\mathcal{J}} p_{u,j}^{UL} + P_C, \tag{16}$$

where ρ_d and $\rho_u \in [0\ 1]$ are the power conversion efficiencies at the BS and the UL users respectively. Apparently, the energy efficiency of the considered system is given by

$$EE = \frac{SE}{P_T}. \tag{17}$$

C. Problem formulation

Notably, the SE increases as the power consumption for transmission increases. To maximize the SE, it is necessary to use all available transmit power. However, this approach may not be ideal for maximizing EE, as EE aims to achieve a balance between SE and power consumption. As a result, SE and EE are in conflict in the moderate and high signal-to-noise ratio (SNR) regimes, leading to a tradeoff between the two metrics. In this subsection, we explore this tradeoff and determine the optimal resource allocation design strategy that strikes the best balance between SE and EE. This tradeoff can be viewed as a multi-objective optimization (MOO) problem given by

$$(P1): \max_{\mathbf{w}_c,\mathbf{w},\mathbf{P},\mathbf{c}} \; SE(\mathbf{w}_c,\mathbf{w},\mathbf{P},\mathbf{c}) \tag{18a}$$

$$\max_{\mathbf{w}_c,\mathbf{w},\mathbf{P},\mathbf{c}} \; EE(\mathbf{w}_c,\mathbf{w},\mathbf{P},\mathbf{c}) \tag{18b}$$

$$\text{s.t. } (C.1): \sum\nolimits_{d\in\mathcal{D}} |\mathbf{w}_d|^2 + |\mathbf{w}_c|^2 \le p_{max}^{DL}, \tag{18c}$$

$$(C.2): \sum\nolimits_{i\in\mathcal{D}} C_i \le R_{\mathrm{c},d}^{DL}, \forall d \in \mathcal{D}, \tag{18d}$$

$$(C.3): C_d \ge 0, \; \forall d \in \mathcal{D} \tag{18e}$$

$$(C.4): R_{d,tot}^{DL} \ge R_{d,min}^{DL}, \forall d \in \mathcal{D}, \tag{18f}$$

$$(C.5): \sum\nolimits_{j\in\mathcal{J}} p_{u,j}^{UL} \le p_{u,max}^{UL}, \forall u \in \mathcal{U}, \tag{18g}$$

$$(C.6): \sum\nolimits_{j\in\mathcal{J}} R_{u,j}^{UL} \ge R_{u,min}^{UL}, \forall l \in \mathcal{U}. \tag{18h}$$

where the constraints $(C.1)$ and $(C.5)$ denote that the transmit power budget available at BS and each u^{th} user which is restricted upto p_{max}^{DL} and $p_{u,max}^{UL}$, respectively, $(C.2)$ and $(C.3)$ ensure that each DL user decodes the common stream successfully, and the constraints $(C.4)$ and $(C.6)$ ensure the QoS for each d^{th} DL and u^{th} UL user such that $R_{d,min}^{DL}$ and $R_{u,min}^{UL}$ are the minimum rate requirement, respectively.

III. Proposed solution

To handle the conflicting objectives in problem (P1), we use the weighted sum method, which converts the MOO problem to single objective optimization (SOO) problems by prioritizing each objective function. The objective function of the SOO problem is given by

$$\mathcal{O}_{_{EE-SE,1}} = \frac{\varrho}{\varphi_{EE}} EE + \frac{(1-\varrho)}{\varphi_{SE}} SE, \tag{19}$$

where ϱ is the trade-off parameter and φ_{EE} and φ_{SE} are the normalization factors. Using the Dinkelbach method [16], the objective function (19) is transformed as

$$\mathcal{O}_{_{EE-SE,2}} = \varphi_{_{SE-EE}} SE - qP_T, \tag{20}$$

where $\varphi_{_{SE-EE}} = (\varrho\varphi_{SE} + (1-\varrho)\varphi_{EE})/(\varphi_{SE}\varphi_{EE})$. By dividing the transformed objective function with $\varphi_{_{SE-EE}}$, (20) is transformed as

$$\mathcal{O}_{_{EE-SE,3}} = SE - \left(qP_T \Big/ (\varphi_{_{SE-EE}}) \right). \tag{21}$$

By replacing the positive constant $q/\varphi_{_{SE-EE}}$ with $\chi/(1-\chi)$, for $0 < \chi < \chi_{EE} < 1$, where $\chi_{EE}/(1-\chi_{EE}) = q\varphi_{EE}/\varphi_{SE}$ and multiplying with $(1-\chi)$, (21) is written as

$$\mathcal{O}_{_{EE-SE,4}} = (1-\chi)SE - \chi P_T, \tag{22}$$

The objective function $\mathcal{O}_{_{EE-SE,4}}$ in equation (22) transforms the SE-EE trade-off problem, with ϱ as the trade-off parameter, into a SE-PT trade-off problem with χ as the trade-off parameter. $\mathcal{O}_{_{EE-SE,4}}$ seeks to maximize SE while minimizing total power consumption. Consequently, the solution to (P1) can be derived from the subsequent SOO problem, as:

$$(P2): \max_{\mathbf{w}_c,\mathbf{w},\mathbf{P},\mathbf{c}} \; \frac{(1-\chi)}{\xi_{SE}} SE - \frac{\chi}{\xi_{PT}} P_T \tag{23a}$$

$$\text{s.t. } (C.1), \ldots, (C.6), \tag{23b}$$

where ξ_{SE} and ξ_{PT} are the normalizing factors, calculated by maximizing SE and minimizing P_T respectively [17]. At $\chi = 0$, the problem (P2) can be simplified to maximize SE, while at $\chi = 1$, the problem reduces to minimizing power consumption. The energy-efficient solution is achieved at optimal χ.

The optimization problem formulated in problem (P3) is non-convex due to the coupling of variables in the objective functions (23a), constraints $(C.2)$, $(C.4)$ and $(C.6)$. In general, no standard mathematical optimization scheme exists to provide optimal global solutions to these non-convex problems in polynomial time. As a compromise, attaining high-quality sub-optimal solutions for the resource allocation problems in (P3) is more appealing. In the sequel, we aim to tackle the non-convexity of (P3) and develop an efficient resource allocation scheme using general convex approximations.

For the sake of simplicity, we adopt matched filter criterion for the m^{th} receive beamformer at the BS [18] such that $\mathbf{z}_m = \mathbf{g}_m^{UL}/||\mathbf{g}_m^{UL}||$. We utilize successive convex approximation approach to design the other optimization variables [19]. Using auxiliary variables $\mu_{\mathrm{c},d}^{DL}$, $\mu_{\mathrm{p},d}^{DL}$ and $\mu_{u,j}^{UL}$ the expressions in (6), (9) and (13) are relaxed as follows

$$\gamma_{\mathrm{c},d}^{DL} \ge \frac{|(\mathbf{g}_d^{DL})^{\mathrm{H}}\mathbf{w}_c|^2}{\mu_{\mathrm{c},d}^{DL}}, \gamma_{\mathrm{p},d}^{DL} \ge \frac{|(\mathbf{g}_d^{DL})^{\mathrm{H}}\mathbf{w}_d|^2}{\mu_{\mathrm{p},d}^{DL}},$$
$$\gamma_{u,j}^{UL} \ge \frac{p_{u,j}^{UL}|\mathbf{g}_u^{UL}\mathbf{z}_u|^2}{\mu_{u,j}^{UL}}, \forall d,u,j \in \mathcal{D},\mathcal{U},\mathcal{J} \tag{24}$$

where

$$\mu_{\mathrm{c},d}^{DL} \ge \sum_{i\in\mathcal{D}} |(\mathbf{g}_d^{DL})^{\mathrm{H}}\mathbf{w}_i|^2 + \sum_{u\in\mathcal{U}}\sum_{j\in\mathcal{J}} p_{u,j}^{UL}|h_{d,u}|^2 + (\sigma_{\mathrm{c},d}^{DL})^2. \tag{25}$$

$$\mu_{\mathrm{p},d}^{DL} \ge \sum_{\substack{i\in\mathcal{D},\\ i\neq d}} |(\mathbf{g}_d^{DL})^{\mathrm{H}}\mathbf{w}_i|^2 + \sum_{u\in\mathcal{U}}\sum_{j\in\mathcal{J}} p_{u,j}^{UL}|h_{d,u}|^2 + (\sigma_d^{DL})^2. \tag{26}$$

$$\mu_{u,j}^{UL} \ge \sum_{(m,n)\in\mathcal{Q}_{u,j}} p_{m,n}^{UL}|\mathbf{g}_m^{UL}\mathbf{z}_m|^2 + \left(P_{SI} + \sigma_{BS}^{UL^2}\right)||\mathbf{z}_u||^2. \tag{27}$$

Although the expressions in (24) are non-convex, by letting $\Xi_u = |\mathbf{g}_u^{UL}\mathbf{z}_u|^2$, they can be transformed into an equivalent affine form using the SCA technique at $\{\mathbf{w}_{\mathrm{c}}^{(i)}, \mathbf{w}_d^{(i)}, p_{u,j}^{UL^{(i)}}, \mu_{\mathrm{c},d}^{DL^{(i)}}, \mu_{\mathrm{p},d}^{DL^{(i)}}$ and $\mu_{u,j}^{UL^{(i)}}\}$ as

$$\frac{2\Re\left(\mathbf{w}_{\mathrm{c}}^{(i)\mathrm{H}}(\mathbf{g}_d^{DL})(\mathbf{g}_d^{DL})^{\mathrm{H}}\mathbf{w}_{\mathrm{c}}\right)}{\mu_{\mathrm{c},d}^{DL^{(i)}}} - \frac{\left|(\mathbf{g}_d^{DL})^{\mathrm{H}}\mathbf{w}_{\mathrm{c}}{}^{(i)}\right|^2 \mu_{\mathrm{c},d}^{DL}}{\mu_{\mathrm{c},d}^{DL^{(i)^2}}} \ge \gamma_{\mathrm{c},d}^{DL}, \tag{28}$$

$$\frac{2\Re\left(\mathbf{w}_d^{(i)\mathrm{H}}(\mathbf{g}_d^{DL})(\mathbf{g}_d^{DL})^{\mathrm{H}}\mathbf{w}_d\right)}{\mu_{\mathrm{p},d}^{DL^{(i)}}} - \frac{\left|(\mathbf{g}_d^{DL})^{\mathrm{H}}\mathbf{w}_d{}^{(i)}\right|^2 \mu_{\mathrm{p},d}^{DL}}{\mu_{\mathrm{p},d}^{DL^{(i)^2}}} \ge \gamma_{\mathrm{p},d}^{DL}, \tag{29}$$

$$\Xi_u \left(\frac{p_{u,j}^{UL^{(i)}}}{\mu_{u,j}^{UL^{(i)}}} + \frac{p_{u,j}^{UL}}{\mu_{u,j}^{UL^{(i)}}} - \frac{p_{u,j}^{UL^{(i)}}\mu_{u,j}^{UL}}{\mu_{u,j}^{UL^{(i)^2}}} \right) \ge \gamma_{u,j}^{UL}. \tag{30}$$

Using the approximations in (28), (29) and (30), the problem (P2) is reformulated as

$$(P3): \max_{\mathbf{w}_c,\mathbf{w},\mathbf{P},\mathbf{c},\boldsymbol{\mu}_c,\boldsymbol{\mu}_p,\boldsymbol{\mu}_u} \frac{(1-\chi)}{\xi_{SE}} SE - \frac{\chi}{\xi_{PT}} P_T \tag{31a}$$

$$\text{s.t. } (C.1), (C.3), (C.5), (28), (29), (30), \tag{31b}$$

$$(C_2.2): \sum\nolimits_{i\in\mathcal{D}} C_i \leq \log_2(1+\gamma_{c,d}^{DL}), \forall d \in \mathcal{D}, \tag{31c}$$

$$(C_2.4): C_d^{DL} + \log_2(1+\gamma_{p,d}^{DL}) \geq R_{d,min}^{DL}, \forall d \in \mathcal{D}, \tag{31d}$$

$$(C_2.6): \sum\nolimits_{j\in\mathcal{J}} R_{u,j}^{UL} \geq \log_2(1+\gamma_{u,j}^{UL}), \forall l \in \mathcal{U}, \tag{31e}$$

where $\boldsymbol{\mu}_c, \boldsymbol{\mu}_p, \boldsymbol{\mu}_u$ are defined as $\{\mu_{c,1}^{DL} \dots \mu_{c,D}^{DL}\}$, $\{\mu_{p,1}^{DL} \dots \mu_{p,D}^{DL}\}$ and $\{\mu_{u,j}^{UL} \dots \mu_{U,J}^{UL}\}$.

The above problem is convex and solved using the standard CVX toolbox. We can gradually improve this lower bound by solving (P3) optimally in an iterative manner. Furthermore, the objective function in problem (P3) increases monotonically, which ensures convergence to a stationary point. The tradeoff parameter χ is adjusted to achieve the desired priority of the objective functions. $\chi = 0$ is used to optimize the SE objective function, while χ_{EE} is used to optimize EE, which can be obtained from (23) = 0, similar to finding q in solving the EE problem. The optimal SE-EE tradeoff problem under the SCA framework is summarized in **Algorithm 1**.

Algorithm 1 Proposed Algorithm

1: Initialize $\mathbf{w}_c^{(i)}$, $\mathbf{w}^{(i)}$, $\mathbf{P}^{(i)}$, $\boldsymbol{\mu}_c{}^{(i)}$, $\boldsymbol{\mu}_p{}^{(i)}$, $\boldsymbol{\mu}_u{}^{(i)}$, $\chi^{(j)}$, j_{max}, i_{max} and $i = j = 1$ and.
2: Evaluate ξ_{SE} and ξ_{PT}.
3: **while** $j \leq j_{max}$ **do**
4: **while** $i \leq i_{max}$ **do**
5: Evaluate $\mathbf{w}_c^{(i+1)}$, $\mathbf{w}^{(i+1)}$, $\mathbf{P}^{(i+1)}$ using problem (P3)
6: Evaluate SE and EE using (15) and (17) respectively
7: **end while**
8: Obtain $\chi^{(j+1)} = SE\xi_{PT}/(SE\xi_{PT} + EE\xi_{SE})$
9: $i \rightarrow i+1$ and $j \rightarrow j+1$
10: **end while**
11: **Output:** χ^*,$\mathbf{w}_c^{(*)}$,$\mathbf{w}^{(*)}$, $\mathbf{P}^{(*)}$.

Let the inner and outer layers of the proposed algorithm converge within Q^{max}, C^{max} SCA iterations which have $a = M_t + DM_t + 3D + 2JU$ variables and $b = 5D + U(2+J) + 1$ affine constraints. Therefore, the computational complexity of the proposed solution for the problem (P3) is $\mathcal{O}(Q^{max}C^{max}ab^2)$ [20].

IV. Results and Discussions

This section presents the performance analysis and effectiveness of the proposed FD-RSMA system and its solution by averaging over more than 100 independent realizations of randomly generated channels via Monte-Carlo simulations. Moreover, we showcase the impact of RSMA on the performance of the considered full-duplex network while comparing it with SDMA. Without loss of generality, we assume that the BS with $M_t = 3$ transmit and $M_r = 2$ receive antennas is located at (0,60m), D = 4 DL users, and U = 2 are distributed randomly circularly centered at $(x_{UL}, 0)$, $x_{UL} = 30$ m and $(x_{DL}, 0)$, $x_{DL} = 30$ m respectively, within a radius of $R_c = 30$ m [21]. The minimum QoS for DL and UL users are set as $R_{d,min}^{DL} = R_{min} = 0.1$ and $R_{u,min}^{UL} = 0.1$ respectively. The available transmit power at BS and the UL users are set as $p_{max}^{DL} = p_{max} = 10$ dB and $p_{u,max}^{UL} = p_{max}^{UL} = 5$ dB and the noise power is as $\sigma_{BS}^{UL^2} = \sigma_d^{DL^2} = -80$dBm, $\forall d$ [3]. Further, the large-scale path-loss (in dB) is followed as $P_{L_i} = P_{L_0}(d_i/d_0)^{-\alpha_i}$, where $P_{L_0} = -30$dB denotes the path-loss at the reference distance of d_0 = 1m, and α_i ($\forall i \in \mathbf{g}_d^{DL}, \mathbf{g}_u^{UL}, \mathbf{F}, h_{d,u}$) represents the path-loss exponent between the BS and the d^{th} DL user, the u^{th} UL user-BS, the SI channel, and the u^{th} UL user-d^{th} DL user links, respectively [19]. Moreover, d_i is the distance of the i^{th} link, and α_i = 2.2 is the path-loss exponents. We assume that small-scale fading for all links follows the Rayleigh distribution [21].

Firstly, the convergence behavior of the outer loop of the proposed iterative solution in **Algorithm 1** and the corresponding convergence of the EE is depicted in Fig. 2. The proposed algorithm converges within 5 iterations as the optimal χ, i.e., the trade-off parameter attains a stationary point. We also highlight the convergence of EE performance w.r.t. corresponding χ. Note that we compare the proposed solution for FD-RSMA with the counterpart FD-SDMA and FD-NOMA schemes. The results validate that FD-RSMA attains substantial improvement compared to FD-SDMA and FD-RSMA, with performance gains of nearly 23.53% and 46.51%, respectively. Factly, the splitting of the messages into sub-messages in RSMA renders a higher degree of freedom in interference management, both cross-interference (SI and UDI) and IUI.

Fig. 3 illustrates the impact of the trade-off parameter, χ on the average EE and SE for the considered FD-RSMA system under different values of R_{min} and p_{max}. Under $\chi = 0$, the BS utilizes the maximum available transmit power to captivate maximum SE which deteriorates overall EE performance. On the other hand, at $\chi = 1$, the objective boils down to the power minimization problem in which power is only used to achieve the given QoS which ultimately results in decreases of both SE and EE. Note that the gradual increase in χ simultaneously balances the obtained SE and the required power leading to an increase in the EE until it reaches the maximum performance. However, a further increase in χ deteriorates the EE as the rate of decrement in power is more than the rate of decrement in SE. This trend persists until the desired QoS is met, causing a saturation point in both EE and SE. Nevertheless, the higher QoS rate enforces the SE and EE to saturate at higher performance. Notably, the increase in transmit power budget experience a lower value of optimal χ and renders better SE and EE performance due to efficient power control.

Fig. 4, we show the impact of the interaction between ω and χ on average EE for both FD and HD-RSMA scenarios. Alternatively, the results in Fig. 4 highlight the determination of optimal χ for EE maximization based on varying RSI coefficients. The increase in ω results in higher SI for UL, leading to a decrease in both SE and EE. Conversely, the HD system remains unaffected by ω due to the absence of self-interference. FD-RSMA outperforms HD-RSMA throughout the results, however, the dominance of FD-RSMA over HD-RSMA diminishes as ω increases. Notably, the performance gain of FD-RSMA over HD-RSMA is quite significant only at

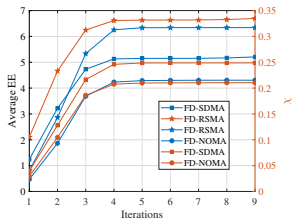

Fig. 2: Convergence of the proposed algorithm.

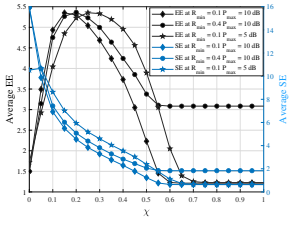

Fig. 3: EE and SE versus the trade-off parameter χ

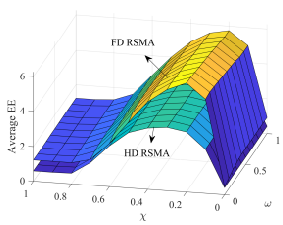

Fig. 4: EE versus trade-off parameter χ and RSI coefficient ω

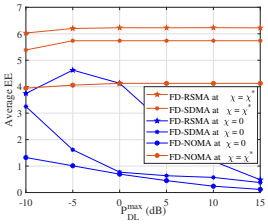

Fig. 5: EE versus available transmit power at BS P_{DL}^{max}

an optimal value of χ (around 0.3).

Finally, Fig. 5 depicts the impact of maximum power available at BS (P_{max}^{DL}) on average EE at optimal χ^* and $\chi = 0$. Note that $\chi = \chi^*$ and $\chi = 0$ correspond to EE performance at optimal trade-off point and SE maximization (EE performance with full transmit power), respectively. Under optimal $\chi = \chi^*$, the EE performance initially increases with transmit power due to an increase in power control flexibility. However, the proposed algorithm maintains the balance between higher SE and lower power which enforces the BS to use a fixed transmit power (optimal power) i.e., fixed EE performance, especially at high P_{DL}^{max}. While for the $\chi = 0$ scenario, with the increase in P_{DL}^{max}, the average EE decreases as the BS utilizes all the available transmit power to maximize SE. The increase in power increases the SE negligibly as IUI dominates at higher transmit power, which significantly decreases the EE with $\chi = 0$. Overall, the proposed FD-RSMA scheme attains better performance than the counterpart SDMA and RSMA.

V. Conclusions

This paper investigated an unconventional RSMA-integrated FD communication system to attain a better EE and SE performance. A MOO problem of the SE-EE trade-off for the considered FD-RSMA system was formulated by jointly optimizing the transmit and receiver beamformer at the BS and power allocation at UL users while guaranteeing the transmit power constraint and minimum rate requirement. Subsequently, an iterative algorithm based on the SCA scheme was adopted to attain a closed-form solution for the formulated non-convex MOO problem. Finally, the simulation results demonstrated the out-performance of considered FD-RSMA over FD-SDMA and FD-NOMA schemes w.r.t SE and EE trade-off. It was shown that the proposed solution attains optimal trade-off point which balances the SE and EE performance effectively. Nevertheless, the results in this work serve as a theoretical performance bound for the FD-RSMA system, and the detailed investigation of a robust FD-RSMA system design under imperfect CSI is left as a future extension of this work.

References

[1] M. Wang, Y. Lin, Q. Tian, and G. Si, "Transfer learning promotes 6G wireless communications: Recent advances and future challenges," *IEEE Trans. Rel*, vol. 70, no. 2, pp. 790–807, Jun. 2021.

[2] Y. Liu *et. al.*, "Evolution of NOMA toward next generation multiple access (NGMA) for 6G," *IEEE J. Sel. Areas Commun.*, vol. 40, no. 4, pp. 1037–1071, 2022.

[3] R. Zhang, Y. Li, C.-X. Wang, Y. Ruan, Y. Fu, and H. Zhang, "Energy-spectral efficiency trade-off in underlaying mobile D2D communications: An economic efficiency perspective," *IEEE Trans. Wireless Commun.*, vol. 17, no. 7, pp. 4288–4301, Jul. 2018.

[4] H. Harada, K. Mizutani, T. Matsumura, T. Kato, and K. Shioiri, "Development of full-duplex cellular system for beyond 5G and 6G systems," in *Proc. PIMRC*, Sep. 2022, pp. 01–05.

[5] M. Chung *et al.*, "Prototyping real-time full duplex radios," *IEEE Commun. Mag.*, vol. 53, no. 9, pp. 56–63, Sep. 2015.

[6] S. Hong, J. Brand, J. I. Choi, M. Jain, J. Mehlman, S. Katti, and P. Levis, "Applications of self-interference cancellation in 5G and beyond," *IEEE Commun. Mag.*, vol. 52, no. 2, pp. 114–121, Feb. 2014.

[7] Y. Mao, *et al.*, "Rate-splitting multiple access: Fundamentals, survey, and future research trends," *IEEE Commun. Surveys Tuts.*, vol. 24, no. 4, pp. 2073–2126, Jul. 2022.

[8] S. Pala, M. Katwe, K. Singh, B. Clerckx, and C.-P. Li, "Spectral-efficient RIS-aided RSMA URLLC: Toward mobile broadband reliable low latency communication (mBRLLC) system," *IEEE Trans. Wireless Commun.*, pp. 1–1, Sep, 2023.

[9] C. De *et al.* , "Subcarrier assignment, user matching and power allocation for weighted sum-rate maximization with RSMA," in *Proc. Global Inf. Infrastruct. Netw. Symp. (GIIS).*, Sep. 2022, pp. 20–24.

[10] G. Zhou, Y. Mao, and B. Clerckx, "Rate-splitting multiple access for multi-antenna downlink communication systems: Spectral and energy efficiency tradeoff," *IEEE Trans. Wireless Commun.*, vol. 21, no. 7, pp. 4816–4828, Jul. 2022.

[11] M. Katwe, K. Singh, B. Clerckx, and C.-P. Li, "Rate-splitting multiple access and dynamic user clustering for sum-rate maximization in multiple RISs-aided uplink mmwave system," *IEEE Trans. Commun*, vol. 70, no. 11, pp. 7365–7383, Nov. 2022.

[12] M. Katwe *et al.*, "Dynamic user clustering and optimal power allocation in UAV-assisted full-duplex hybrid NOMA system," *IEEE Trans. Wireless Commun.*, vol. 21, no. 4, pp. 2573–2590, Nov. 2022.

[13] S. Khisa *et al.*, "Full duplex cooperative rate splitting multiple access for a MISO broadcast channel with two users," *IEEE Commun. Lett.*, vol. 26, no. 8, pp. 1913–1917, Aug. 2022.

[14] B. Matthiesen *et.al.*, "Globally optimal spectrum- and energy-efficient beamforming for rate splitting multiple access," *IEEE Trans. Signal Process.*, vol. 70, pp. 5025–5040, Oct. 2022.

[15] M. Katwe, K. Singh, B. Clerckx, and C.-P. Li, "Improved spectral efficiency in STAR-RIS aided uplink communication using rate splitting multiple access," *IEEE Trans. Wireless Commun.*, pp. 1–1, Jan. 2023.

[16] S. Poornima and A. V. Babu, "Power adaptation for enhancing spectral efficiency and energy efficiency in multi-hop full duplex cognitive wireless relay networks," *IEEE Trans. Mobile Comput.*, vol. 21, no. 6, pp. 2143–2157, Jun. 2022.

[17] H. Al-Obiedollah *et. al.*, "Spectral-energy efficiency trade-off-based beamforming design for MISO non-orthogonal multiple access systems," *IEEE Trans. Wireless Commun.*, vol. 19, no. 10, pp. 6593–6606, 2020.

[18] Y. Sun, D. W. K. Ng, J. Zhu, and R. Schober, "Robust and secure resource allocation for full-duplex MISO multicarrier NOMA systems," *IEEE Trans. Commun*, vol. 66, no. 9, pp. 4119–4137, Sep. 2018.

[19] A. Khalili, S. Zargari, Q. Wu, D. W. K. Ng, and R. Zhang, "Multi-objective resource allocation for IRS-aided SWIPT," *IEEE Wireless Commun. Lett.*, vol. 10, no. 6, pp. 1324–1328, Jun. 2021.

[20] I. Polik *et al.* ", *Interior Point Methods for Nonlinear Optimization*. Berlin, Heidelberg: Springer Berlin Heidelberg, 2010, pp. 215–276.

[21] K. singh *et al.*, "Resource optimization in full duplex non-orthogonal multiple access systems," *IEEE Trans. Wireless Commun.*, vol. 18, no. 9, pp. 4312–4325, Sep. 2019.